Instrumentation Science and Technology, 41:545–555, 2013

ISSN: 1073-9149 print/1525-6030 online
DOI: 10.1080/10739149.2013.798808

DETECTION OF FORMATION AND DISINTEGRATION OF MICELLES BY OBLIQUE-INCIDENCE REFLECTIVITY DIFFERENCE MICROSCOPY

Yung-Shin Sun,[1,2] Juntao Luo,[3,4] Kit S. Lam,[3,5] and X. D. Zhu[2]

[1]*Department of Physics, Fu-Jen Catholic University, New Taipei City, Taiwan*
[2]*Department of Physics, University of California at Davis, Davis, California, USA*
[3]*Department of Biochemistry and Molecular Medicine, School of Medicine, University of California at Davis, Sacramento, California, USA*
[4]*Department of Pharmacology, Upstate Cancer Research Institute, State University of New York, Upstate Medical University, Syracuse, New York, USA*
[5]*Division of Hematology and Oncology, Department of Internal Medicine, School of Medicine, University of California at Davis, Sacramento, California, USA*

□ *An oblique-incidence reflectivity difference (OI-RD) scanning microscope was developed for label-free detection of the formation and disintegration of micelles upon solid substrates. Micelles are made of polymers with hydrophilic heads in contact with the surrounding solvent and hydrophobic tails in the micelle center. This characteristic makes them very efficient drug carriers. Streptavidin molecules were first printed on glass slides for capturing biotinylated polymers. Micelles were formed when the concentration of polymers was higher than a critical value. The formation of micelles resulted in an increase in the oblique-incidence reflectivity difference signals. As the concentration of polymers decreased below the critical value, micelles were disintegrated, and a corresponding decrease in the oblique-incidence reflectivity difference signals was observed. This microscope was employed for the real-time monitoring of the formation and disintegration of two different micelles. The critical concentration above which micelles were formed was determined to be around 0.0006 mg/mL for micelles made of* $PEG^{5K}CA_8$ *polymers. The results suggest that this microscope would have practical application in testing the efficiency and durability of micellar drug carriers.*

Keywords critical concentration, drug carrier, micelle, oblique-incidence reflectivity difference microscope

INTRODUCTION

In order to efficiently deliver drugs with low solubility to targets inside a cell, various drug carriers such as liposomes,[1] microparticles,[2] nano-associates,[3]

Address correspondence to Yung-Shin Sun, Fu-Jen Catholic University, No.510, Zhongzheng Rd., Xinzhuang Dist., New Taipei City 24205, Taiwan (R.O.C.). E-mail: 089957@mail.fju.edu.tw

nanoparticles,[4] drug-polymer conjugates,[5] and polymeric micelles[6,7] have been developed. Among these drug carriers, polymeric micelles are of particular interest because of their capability of both drug delivery and controllable targeting and release. A typical micelle is made of amphiphilic block copolymers with hydrophilic heads in contact with the surrounding solvent and hydrophobic tails in the micelle center. This core-shell structure enables micelles to serve as efficient carries since the hydrophobic core creates a microenvironment surrounding lipophilic drugs, while the hydrophilic shell provides a stable interface between the core and the aqueous solvent.[8,9] Micelles are approximately spherical in shape with a generally small size (diameter < 100 nm). Their shape and size depend on the geometry of the polymers and environmental conditions such as polymer concentration, pH, temperature, and ionic strength. The distribution and transport of drug-loaded micelles in a living system are mainly determined by their size and surface properties, and less by the nature of embedded drugs. Therefore, the use of specific polymeric micelles with a controllable size is crucial to efficiently load and deliver drugs. Micelles can be surface-conjugated with certain moieties such as saccharides,[10,11] folate,[12,13] peptides,[14] and biotin[15,16] for specific targeting. Using biotin as an example, the recognizing ligands such as monoclonal antibodies[17] conjugated with streptavidin can be administered first so that the antibody can seek out and attach to a specific antigen. The following administration (introduction) of biotinylated drug-loaded micelles can then be delivered to the antigen site through a strong biotin-streptavidin interaction. In addition to targeting and delivery, it may be practical to develop novel stimuli-responsive micelles for active drug release. Thermo-[18–21] and pH-[22,23] triggered micelles have been reported to serve for controllable drug release.

Traditionally, the shape (formation and disintegration) of micelles was monitored using the so-called tensiometers which measure the surface and interfacial tensions. Such measurements often require complicated and expensive instruments, such as commercially available Sigma 700/701 tensiometers. Fluorescence labeling has also been used to determine the shape of micelles with very high sensitivities.[24–26] However, different labeling agents (such as fluorophores, nanoparticles, and quantum dots) have different efficiencies, and it is not easy to compare them. Also, labeling is always expensive as well as laborious.

In this article, the use of an oblique-incidence reflectivity difference (OI-RD) microscope is demonstrated to observe the label-free formation and disintegration of biotinylated micelles in real time. OI-RD microscopy, the most sensitive form of optical elliposometry, measures the difference in reflectivity change (both magnitude and phase) between *p*- and *s*-polarized components of an optical beam. Such a difference is related to the thickness and dielectric constant of surface-immobilized biomolecules.

Therefore it is suitable for monitoring the shape of micelles upon solid substrates. In the past, oblique-incidence reflectivity difference microscopes have been applied to label-free detection of various biomolecular interactions in a microarray format.[27–31] In addition to detection of the shape of micelles, the OI-RD microscope was used to determine the critical concentration above which micelles were formed.

MATERIALS AND METHODS

Protein Targets and Biotinylated Micelles

Unlabeled streptavidin tetramers were purchased from Jackson ImmunoResearch Laboratories (West Grove, PA) and dissolved in 1 × PBS into a printing solution of 0.5 mg/mL. Two different micelles (composed of $PEG^{5K}CA_8$ polymers and cross-linked polymers, respectively) were synthesized as described in references.[32–34] Mixtures of inert polymers and biotinylated polymers at different loading ratios (polymer-biotin: polymer-inert = 1:5, 1:10, 1:20, and 1:40) were prepared. The structures of $PEG^{5K}CA_8$ polymer (non cross-linked telodendrimer)-biotin and cross-linked polymer (catechol-boronic acid cross-linked polymer)-biotin are shown in Figure 1.

Preparation of Target Microarrays

Using an OmniGrid 100 contact-printing arrayer (Digilab, Holliston, MA, USA), two duplicates of streptavidin were printed on epoxy-coated glass slides for capturing biotinylated micelles. The microarray-bearing slides were stored as printed in slide boxes for at least 24 hr before further processing.

OI-RD Microscope

The formation-disintegration curves of micelles were acquired using an oblique-incidence reflectivity difference microscope. The scanning microscope employs a He-Ne laser at a wavelength (λ) of 633 nm for illumination. The complex differential reflectivity change ($\Delta_p - \Delta_s$) across a microarray-covered glass surface is measured.[35] The physical properties of a surface-bound molecular layer on a glass surface are related to $\Delta_p - \Delta_s$ by

$$\Delta_p - \Delta_s \cong -i\left[\frac{4\pi\varepsilon_s(\tan\varphi_{inc})^2\cos\varphi_{inc}}{\varepsilon_0^{1/2}(\varepsilon_s-\varepsilon_0)\left(\varepsilon_s/\varepsilon_0-(\tan\varphi_{inc})^2\right)}\right] \times \frac{(\varepsilon_d-\varepsilon_s)(\varepsilon_d-\varepsilon_0)}{\varepsilon_d}\left(\frac{d}{\lambda}\right),^{[28,31,36]} \quad (1)$$

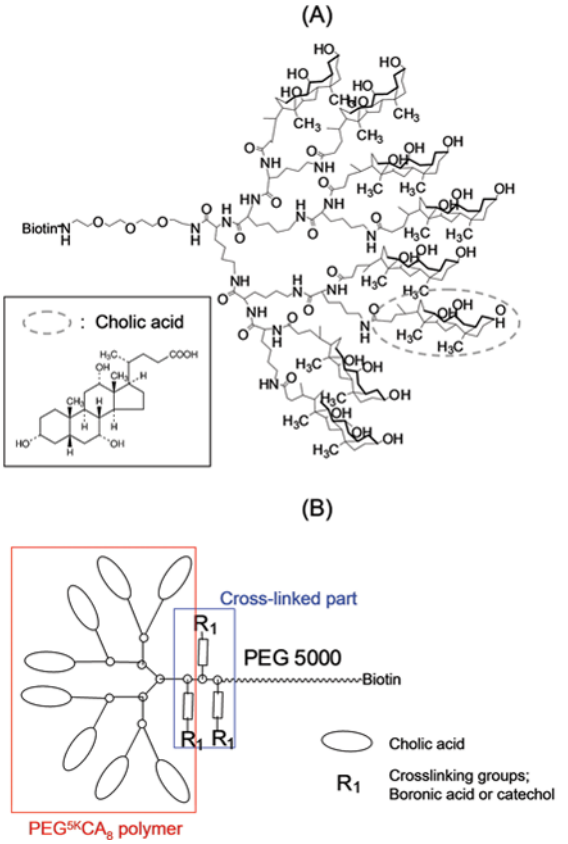

FIGURE 1 Chemical structures of (A) $PEG^{5K}CA_8$ polymer (non cross-linked telodendrimer)-biotin and (B) cross-linked polymer (catechol-boronic acid cross-linked polymer)-biotin. Inset in (A) shows the chemical structure of cholic acid. (color figure available online.)

where φ_{inc} is the incident angle of illumination; ε_0, ε_d, and ε_s are the respective optical constants of the aqueous ambient, the molecular layer (e.g., captured biomolecular probes), and the glass slide at $\lambda = 633$ nm; and d is the thickness of the molecular layer. A single photodiode detector is used for measuring the OI-RD signals (in terms of $\Delta_p - \Delta_s$). To enable two-dimensional and high-speed scanning, two piezo-nano-positioning (PI) encoded, linear stages were employed. For real-time, kinetic curve measurements, OI-RD signals from spots and their neighboring bare substrates were monitored over time. By repeatedly moving two stages and focusing the laser beam on desired locations, the real-time curves of all targets were acquired. The referenced optical signal of a target was acquired by subtracting the averaged signal of the two adjacent bare substrates from the signal of the target.

Experimental Procedures

Before assembling the sample cartridge, a microarray-bearing slide was immersed in 1 × PBS overnight to remove excess unbound targets and buffer precipitates. After assembling, the slide printed with molecular targets was first washed twice with a flow of 1 × PBS at a rate of 5 mL/min. It was subsequently blocked for 10 min with a solution of BSA at 0.5 mg/mL and washed again with fresh 1 × PBS for 5 min. To acquire real-time curves, the flow cell was first rapidly filled with the reagent containing micelles at 0.05 mg/mL at a rate of 5 mL/min and then the flow rate was slowed down to 0.01 mL/min. To observe the disintegration, the reagent solution was rapidly replaced with fresh 1 × PBS or micellar solutions at desired concentrations at a flow rate of 5 mL/min and then the flow rate was reduced to 0.01 mL/min.

RESULTS AND DISCUSSION

Figure 2 illustrates the overall experimental procedure. First, streptavidin molecules were printed on a bare glass slide ((A) and (B)). Then after polymers were brought to the glass surface, polymer-biotin was bound to immobilized streptavidin through a strong biotin-streptavidin interaction, and micelles were formed (C). After the reagent was replaced with 1 × PBS or polymers at lower concentrations, the disintegration of micelles occurred (D). Figure 3 shows the formation-disintegration curves of $PEG^{5K}CA_8$ micelles with different polymer-biotin to polymer-inert loading ratios. As shown in Eq. (1), the changes in thickness (d) and dielectric constant

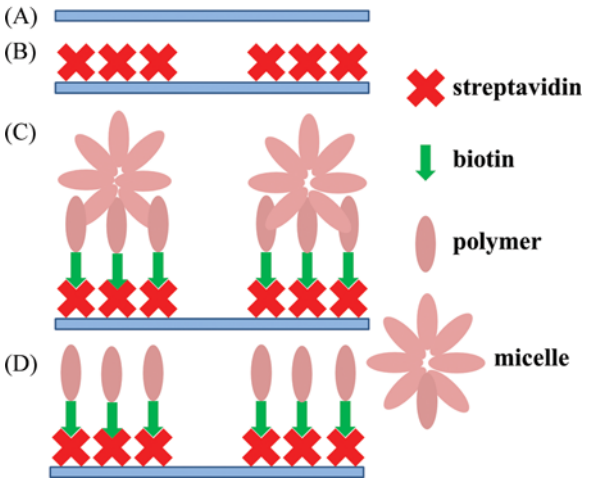

FIGURE 2 (A) Bare glass substrate, (B) printed streptavidin spots, (C) formation of micelles, and (D) disintegration of micelles. (color figure available online.)

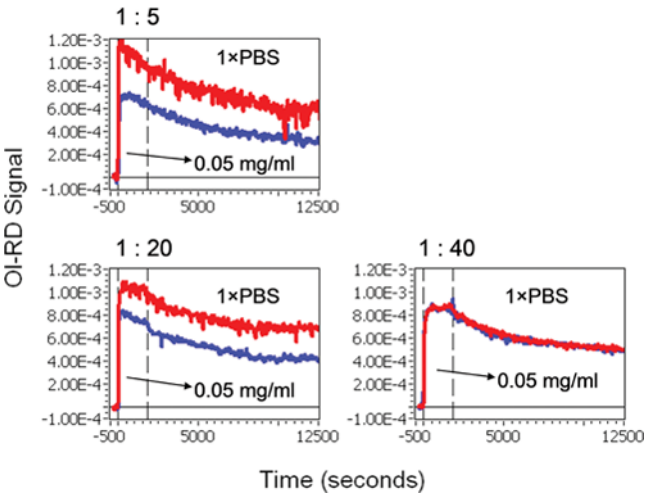

FIGURE 3 Formation-disintegration curves of micelles composed of $PEG^{5K}CA_8$ polymers at different loadings. Two curves represent signals from two duplicated spots. Concentration of mixed polymers used was 0.05 mg/mL. After 1800 s, 1 × PBS buffer replaced the mixtures and disintegration occurred. All disintegration curves were fitted to the Langmuir one-site model with k_{off} listed in Table 1. (color figure available online.)

(ε_d) of micelles contributed to the OI-RD signal. Assuming that the dielectric constant was unchanged, the OI-RD signal was proportional to the thickness of micelles, which is larger when micelles were formed and smaller when they were disintegrated. There are two curves in each figure representing signals from two duplicated streptavidin spots. The polymer solution mixture (at 0.05 mg/mL) was brought to the streptavidin microarray at $t = 0$ (marked by the first dashed line), and then the solution was replaced with fresh 1 × PBS at $t = 1800$ s (marked by the second dashed line) for another 3 hr. The mixture of inert polymers and biotinylated polymers formed micelles with their biotin tags attached to surface-immobilized streptavidin. For a loading ratio = 1:5, the equilibrium was reached and the disintegration occurred before the injection of 1 × PBS, which probably occurred because too many biotin molecules (and micelles) bound rapidly to surface streptavidin within the first few minutes but some conformational changes occurred right after that point and thus caused the decrease in signals. All disintegration curves were fitted to the Langmuir one-site

TABLE 1 Off-rate (Disintegration Rate) of $PEG^{5K}CA_8$ Micelles with Different Loadings

k_{off} $(s)^{-1}$	1 : 5	1 : 20	1 : 40
First spot	3.81×10^{-5}	2.61×10^{-5}	3.58×10^{-5}
Second spot	4.76×10^{-5}	3.83×10^{-5}	3.47×10^{-5}

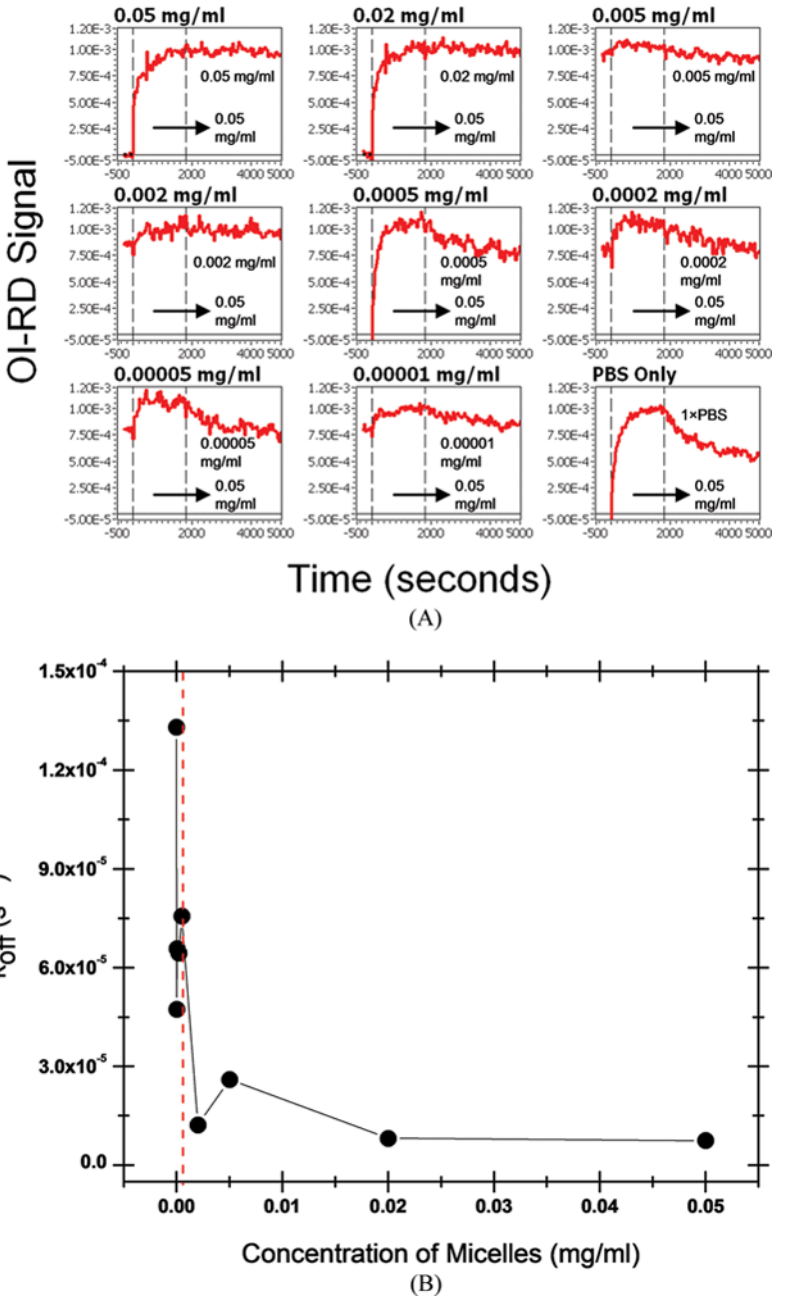

FIGURE 4 (A) Disintegration curves of $PEG^{5K}CA_8$ micelles (loading ratio = 1:40) at different micellar concentrations (from 0–0.05 mg/mL). Concentration of mixed polymers used was 0.05 mg/mL. (B) Off-rate (disintegration rate) vs. micellar concentration at the disintegration phase. The dashed line corresponds to the estimated critical concentration, which is approximately 0.0006 mg/mL. (color figure available online.)

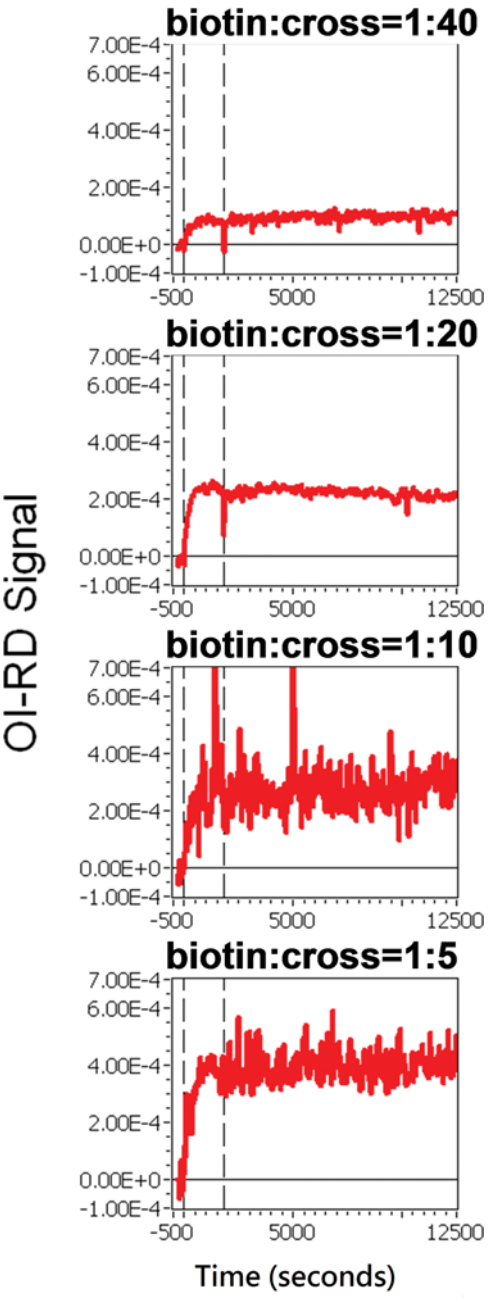

FIGURE 5 Formation-disintegration curves of micelles composed of cross-linked polymers at different loadings. Concentration of mixed polymers used was 0.05 mg/mL. After 1800 s, 1 × PBS buffer replaced the mixtures and disintegration occurred. From top to bottom, polymer-biotin: polymer-inert = 1:40, 1:20, 1:10, and 1:5. (color figure available online.)

model[31,37] with the off-rate (dissociation rate) k_{off} listed in Table 1. The disintegration rates for all three mixtures were in the range of $3 \sim 5 \times 10^{-5}\,(\mathrm{s})^{-1}$. Also, the disintegration (or dissociation) seemed to reach equilibrium after a long time period (up to 12 hr, data not shown). To find the critical concentration above which micelles were formed, disintegration curves of $PEG^{5K}CA_8$ micelles (loading ratio = 1:40) were measured at different micellar concentrations (from 0–0.05 mg/mL) as shown in Figure 4A. During formation, the concentration of mixed polymers used was 0.05 mg/mL. As illustrated in Figure 4), the Langmuir one-site model-fitted off-rate was plotted against the micellar concentration at disintegration phase. The off-rate decreased as the micellar concentration increased, and stable micelles formed (i.e., no clear disintegration was observed) at concentrations higher than 0.002 mg/mL. The estimated critical concentration for these $PEG^{5K}CA_8$ micelles was approximately 0.0006 mg/mL, as indicated by the dashed line in Figure 4B.

To test the feasibility of this OI-RD microscope, different loadings of cross-linked polymers were prepared for comparison with the original $PEG^{5K}CA_8$ micelles. Figure 5 shows the formation-disintegration curves of cross-linked micelles with different loadings. During formation, the concentration of mixed polymers used was 0.05 mg/mL. After 1800 s, 1 × PBS buffer replaced the mixtures and disintegration occurred. Regardless of the loading, no obvious disintegration (or dissociation) was observed in cross-linked micelles, which suggests that cross-linked polymers formed more stable micelles than $PEG^{5K}CA_8$ polymers. However, this might be a drawback for such cross-linked micelles since it would be difficult to effectively release drugs surrounded and carried by them.

CONCLUSIONS

In this article, the formation and disintegration curves of two different micelles were observed and studied using an oblique-incidence reflectivity difference microscope. The critical concentration of $PEG^{5K}CA_8$ micelles was measured to be around 0.0006 mg/mL, and no obvious disintegration of cross-linked micelles was observed. The results indicate that $PEG^{5K}CA_8$ micelles above the critical concentration were stable without disintegration. Therefore, they are suitable for loadings of drugs and for studying how to efficiently control the process of targeting and releasing. Moreover, this microscope was demonstrated to be applicable to studying the efficiency of micellar drug carriers.

ACKNOWLEDGMENT

The authors thank financial supports from NIH-R01-HG003827 (X.D. Zhu) and Taiwan NSC 101-2112-M-030-003-MY3 (Y.S. Sun).

REFERENCES

1. Lasic, D. D. Doxorubicin in sterically stabilized liposomes. *Nature* **1996**, *380*(6574), 561–562.
2. Spenlehauer, G.; Spenlehauer-Bonthonneau, F.; Thies, C. Biodegradable microparticles for delivery of polypeptides and proteins. *Prog. Clin. Biol. Res.* **1989**, *292*, 283–291.
3. Akiyoshi, K.; Kobayashi, S.; Shichibe, S.; et al. Self-assembled hydrogel nanoparticle of cholesterol-bearing Pullulan as a carrier of protein drugs: Complexation and stabilization of insulin. *J. Control Release* **1998**, *54*(3), 313–320.
4. Allemann, E.; Leroux, J. C.; Gurny, R.; Doelker, E. In vitro extended-release properties of drug-loaded poly(DL-lactic acid) nanoparticles produced by a salting-out procedure. *Pharm. Res.* **1993**, *10*(12), 1732–1737.
5. Duncan, R. Drug-polymer conjugates: Potential for improved chemotherapy. *Anticancer Drugs* **1992**, *3*(3), 175–210.
6. Jones, M.; Leroux, J. Polymeric micelles - A new generation of colloidal drug carriers. *Eur. J. Pharm. Biopharm.* **1999**, *48*(2), 101–111.
7. Kataoka, K.; Harada, A.; Nagasaki, Y. Block copolymer micelles for drug delivery: Design, characterization and biological significance. *Adv. Drug. Deliv. Rev.* **2001**, *47*(1), 113–131.
8. La, S. B.; Okano, T.; Kataoka, K. Preparation and characterization of the micelle-forming polymeric drug indomethacin-incorporated poly(ethylene oxide)-poly(beta-benzyl L-aspartate) block copolymer micelles. *J. Pharm. Sci.* **1996**, *85*(1), 85–90.
9. Liu, X. M.; Yang, Y. Y.; Leong, K. W. Thermally responsive polymeric micellar nanoparticles self-assembled from cholesteryl end-capped random poly(N-isopropylacrylamide-co-N,N-dimethylacrylamide): synthesis, temperature-Sensitivity, and morphologies. *J. Colloid Interface Sci.* **2003**, *266*(2), 295–303.
10. Joralemon, M. J.; Murthy, K. S.; Remsen, E. E.; Becker, M. L.; Wooley, K. L. Synthesis, characterization, and bioavailability of mannosylated shell cross-linked nanoparticles. *Biomacromolecules* **2004**, *5*(3), 903–913.
11. Nagasaki, Y.; Yasugi, K.; Yamamoto, Y.; Harada, A.; Kataoka, K. Sugar-installed block copolymer micelles: Their preparation and specific interaction with lectin molecules. *Biomacromolecules* **2001**, *2*(4), 1067–1070.
12. Pan, D.; Turner, J. L.; Wooley, K. L. Folic acid-conjugated nanostructured materials designed for cancer cell targeting. *Chem. Commun. (Camb.)* **2003**(19), 2400–2401.
13. Bae, Y.; Nishiyama, N.; Kataoka, K. In vivo antitumor activity of the folate-Conjugated pH-sensitive polymeric micelle selectively releasing adriamycin in the intracellular acidic compartments. *Bioconjug. Chem.* **2007**, *18*(4), 1131–1139.
14. Oba, M.; Fukushima, S.; Kanayama, N.; et al. Cyclic RGD peptide-conjugated polyplex micelles as a targetable gene delivery system directed to cells possessing alphavbeta3 and alphavbeta5 integrins. *Bioconjug. Chem.* **2007**, *18*(5), 1415–1123.
15. Cheng, C.; Wei, H.; Shi, B. X.; et al. Biotinylated thermoresponsive micelle self-assembled from double-hydrophilic block copolymer for drug delivery and tumor target. *Biomaterials* **2008**, *29*(4), 497–505.
16. Wang, X.; Liu, L.; Luo, Y.; Zhao, H. Bioconjugation of biotin to the interfaces of polymeric micelles via in situ click chemistry. *Langmuir* **2009**, *25*(2), 744–750.
17. Nobs, L.; Buchegger, F.; Gurny, R.; Allemann, E. Biodegradable nanoparticles for direct or two-step tumor immunotargeting. *Bioconjug. Chem.* **2006**, *17*(1), 139–145.
18. Kim, I. S.; Jeong, Y. I.; Cho, C. S.; Kim, S. H. Thermo-responsive self-assembled polymeric micelles for drug delivery in vitro. *Int. J. Pharm.* **2000**, *205*(1–2), 165–172.
19. Kim, I. S.; Jeong, Y. I.; Lee, Y. H.; Kim, S. H. Drug release from thermo-responsive self-assembled polymeric micelles composed of cholic acid and poly(N-isopropylacrylamide). *Arch. Pharm. Res.* **2000**, *23*(4), 367–373.
20. Chung, J. E.; Yokoyama, M.; Okano, T. Inner core segment design for drug delivery control of thermo-responsive polymeric micelles. *J. Control Release* **2000**, *65*(1–2), 93–103.
21. Chung, J. E.; Yokoyama, M.; Yamato, M.; Aoyagi, T.; Sakurai, Y.; Okano, T. Thermo-responsive drug delivery from polymeric micelles constructed using block copolymers of poly(N-isopropylacrylamide) and poly(butylmethacrylate). *J. Control Release* **1999**, *62*(1–2), 115–127.

22. Lee, E. S.; Na, K.; Bae, Y. H. Super pH-sensitive multifunctional polymeric micelle. *Nano Lett.* **2005**, *5*(2), 325–329.
23. Gillies, E. R.; Jonsson, T. B.; Frechet, J. M. Stimuli-responsive supramolecular assemblies of linear-dendritic copolymers. *J. Amer. Chem. Soc.* **2004**, *126*(38), 11936–11943.
24. Gao, L.; Zhao, L.; Huang, X.; Xu, B.; Yan, Y.; Huang, J. A surfactant type fluorescence probe for detecting micellar growth. *J. Colloid Interf. Sci.* **2011**, *354*(1), 256–260.
25. Lifeng, C.; Gochin, M. Colloidal aggregate detection by rapid fluorescence measurement of liquid surface curvature changes in multiwell plates. *J. Biomol. Screen* **2007**, *12*(7), 966–971.
26. Goddard, E. D.; Turro, N. J.; Kuo, P. L.; Ananthapadmanabhan, K. P. Fluorescence probes for critical micelle concentration determination. *Langmuir* **1985**, *1*(3), 352–355.
27. Landry, J. P.; Sun, Y. S.; Guo, X. W.; Zhu, X. D. Protein reactions with surface-bound molecular targets detected by oblique-incidence reflectivity difference microscopes. *Appl. Opt.* **2008**, *47*(18), 3275–3288.
28. Zhu, X.; Landry, J. P.; Sun, Y. S.; Gregg, J. P.; Lam, K. S.; Guo, X. Oblique-incidence reflectivity difference microscope for label-free high-throughput detection of biochemical reactions in a microarray format. *Appl. Opt.* **2007**, *46*(10), 1890–1895.
29. Landry, J. P.; Zhu, X. D.; Gregg, J. P. Label-free detection of microarrays of biomolecules by oblique-incidence reflectivity difference microscopy. *Opt. Lett.* **2004**, *29*(6), 581–583.
30. Sun, Y. S.; Landry, J. P.; Fei, Y. Y.; et al. Macromolecular scaffolds for immobilizing small molecule microarrays in label-free detection of protein-ligand interactions on solid support. *Anal. Chem.* **2009**, *81*(13), 5373–5380.
31. Sun, Y. S.; Landry, J. P.; Fei, Y. Y.; et al. Effect of fluorescently labeling protein probes on kinetics of protein-ligand reactions. *Langmuir* **2008**, *24*(23), 13399–13405.
32. Li, Y.; Xiao, K.; Luo, J.; et al. Well-defined, reversible disulfide cross-linked micelles for on-demand paclitaxel delivery. *Biomaterials* **2011**, *32*(27), 6633–6645.
33. Xiao, K.; Li, Y.; Luo, J.; et al. The effect of surface charge on in vivo biodistribution of PEG-oligocholic acid based micellar nanoparticles. *Biomaterials* **2011**, *32*(13), 3435–3446.
34. Luo, J.; Xiao, K.; Li, Y.; et al. Well-defined, size-tunable, multifunctional micelles for efficient paclitaxel delivery for cancer treatment. *Bioconjug. Chem.* **2010**, *21*(7), 1216–1224.
35. Thomas, P.; Nabighian, E.; Bartelt, M. C.; Fong, C. Y.; Zhu, X. D. An oblique-incidence optical reflectivity difference and LEED study of rare-gas growth on a lattice-mismatched metal substrate. *Appl. Phys. A* **2004**, *79*, 131–137.
36. Zhu, X. D. Oblique-incidence optical reflectivity difference from a rough film of crystalline material. *Phys. Rev. B* **2004**, *69*(115407), 1–5.
37. Morton, T. A.; Myszka, D. G.; Chaiken, I. M. Interpreting complex binding kinetics from optical biosensors: A comparison of analysis by linearization, the integrated rate equation, and numerical integration. *Anal. Biochem.* **1995**, *227*(1), 176–185.